

underlying topological structure inherent in the training data. The proposed method was used to model the spatial structure of remotely sensed soil moisture distributions obtained from the southern Great Plains near Oklahoma. It was shown that the SOFM is capable of preserving the second-order statistical properties of 21 204 pixels with as little as 49 neurons.

In the form used here, one may think of the SOFM as representing a data manifold using a finite number of reference vectors as done by general vector quantization algorithms. Planned extensions of the methodology presented here are based on using as input the soil moisture at a given location and at neighboring locations as input to an SOFM. Similar soil moisture distribution would thus be mapped to a single neuron (or neurons spatially adjacent on the grid), and a different local distribution of soil moisture would be mapped to a more distant neuron (on the grid). Potentially, this would allow for differentiation of vegetation and soil characteristics over small distances.

REFERENCES

- [1] C. O. Justice, J. R. G. Townshend, and V. L. Kalb, "Representation of vegetation by continental data sets derived from NOAA-AVHRR data," *Int. J. Remote Sensing*, vol. 12, pp. 999–1021, 1991.
- [2] D. Entekhabi and P. S. Eagleson, "Land surface hydrology parameterization for atmospheric general circulation models including subgrid scale spatial variability," *J. Climate*, vol. 2, pp. 816–831, 1989.
- [3] K. R. Bell, B. J. Blanchard, T. J. Schumge, and M. W. Witzck, "Analysis of surface moisture variations within large-field sites," *Water Resour. Res.*, vol. 16, no. 4, pp. 796–810, 1980.
- [4] T. Kohonen, "Self-organized formation of topologically correct feature maps," *Biol. Cybern.*, vol. 43, pp. 59–69, 1982.
- [5] ———, *Self Organizing Maps*. Berlin, Germany: Springer-Verlag, 1995.
- [6] H. Ritter and K. Schulten, "On the stationary state of Kohonen's self-organizing sensory mapping," *Biol. Cybern.*, vol. 54, pp. 99–106, 1986.
- [7] T. J. Jackson, D. M. Le Vine, C. T. Swift, T. J. Schumge, and F. R. Schiebe, "Large area mapping of soil moisture using the ESTAR passive microwave radiometer in Washita '92," *Remote Sens. Environ.*, vol. 54, pp. 27–37, 1995.
- [8] P. B. Allen and J. W. Naney, "Hydrology of the little Washita River Watershed, Oklahoma: Data and analysis," USDA Tech. Rep. ARS-90, 1991.
- [9] Z. Hu, S. Islam, and Y. Cheng, "Statistical characterization of remotely sensed soil moisture images," *Remote Sens. Environ.*, vol. 61, pp. 310–318, 1997.
- [10] I. Rodriguez-Iturbe, D. Entekhabi, and R. L. Bras, "Nonlinear dynamics of soil moisture at climate scales," *Water Resour. Res.*, vol. 27, no. 8, pp. 1899–1915, 1991.

Effects of Snow Crystal Shape on the Scattering of Passive Microwave Radiation

J. L. Foster, D. K. Hall, A. T. C. Chang,
A. Rango, W. Wergin, and E. Erbe

Abstract—In this study, a discrete dipole scattering model is used to measure the passive microwave radiation scattered by snow particles having different shapes and sizes. The model results demonstrate that the shape of the snow crystal is insignificant in scattering microwave energy in the 37-GHz region of the spectrum.

Index Terms—Crystals, electron microscope, modeling, scattering, shape, snow.

I. INTRODUCTION

No two snow crystals look exactly the same because their histories are different. Precipitating snow crystals grow into forms according to how water molecules fit together as they fall through the atmosphere and encounter different temperature, pressure, and humidity conditions. Impurities or defects on the surface of the crystals affect their growth by helping them to attract water vapor more efficiently. The crystals may take the form of plates, columns, needles, or dendrites, all of which are based on a hexagonal lattice structure. Competition for water vapor plays a big role in determining the shape of the falling crystals [1]. This is also the case for snow crystals that survive their fall to the ground, where the process of constructive metamorphism increases their size and alters their shape. In addition, the constant jostling of the crystals within the snowpack (destructive metamorphism) results in shapes having fewer protuberances.

Microwave emission from a layer of snow over a ground medium consists of contributions from the snow itself and from the underlying ground. Both contributions are governed by the transmission and reflection properties of the air–snow and snow–ground boundaries and by the absorption/emission and scattering properties of the snow layer. Snow crystals scatter part of the cold sky radiation, reducing the upwelling radiation, as measured with a radiometer [2]. The deeper the snow, the more crystals are available to scatter the upwelling microwave energy, and thus it is possible to estimate the depth of the snow as well as the snow water equivalent (SWE).

Presently, a number of microwave algorithms are available to evaluate and retrieve snow cover and snow depth for specific regions and specific seasonal conditions. These algorithms have been derived from research using a combination of microwave sensors onboard satellites, aircraft, and trucks, as well as *in situ* field studies. However, most of the attention in algorithm development has been directed toward the effects of snow crystal size in scattering microwave energy, but crystal size alone does not account for all of the scattering or energy redistribution. Relatively little effort has been given to the role that crystal shape plays in this regard.

Manuscript received April 13, 1998; revised July 17, 1998.

J. L. Foster, D. K. Hall, and A. T. C. Chang are with the Hydrological Sciences Branch, Laboratory for Hydrological Sciences, NASA Goddard Space Flight Center, Greenbelt, MD 20771 USA (e-mail: jfoster@glacier.gsfc.nasa.gov).

A. Rango, W. Wergin, and E. Erbe are with the Hydrology Laboratory, Agricultural Research Service, U.S. Department of Agriculture, Beltsville, MD 20705 USA.

Publisher Item Identifier S 0196-2892(99)01180-8.

The lack of precise information about snow crystal size, shape, and packing characteristics is compensated for by using an average size, an assumed shape, and random crystal orientations in the radiative transfer equations used to calculate energy transfer through the snowpack. It is not known whether a significant error is induced in solving the radiative transfer equations by making these assumptions and using averages; however, it has been demonstrated that, if the crystals size differs significantly from the averages, poor (SWE) values will result [3]. A better understanding of the physics of snow and how microwave energy interacts with snow crystals is needed to make the snow/microwave algorithms more reliable. In developing these algorithms, it is important to determine the amount of microwave energy that is being transferred from the ground through the snowpack.

For this paper, a particle scattering model was used to calculate the extinction efficiency and scattering of different crystal shapes. This information will be valuable for determining whether the shape of the snow crystal is an important enough parameter to be accounted for in modeling the radiative transfer of microwave energy through snowpacks.

In conjunction with the modeling, snow crystals were collected from field sites and brought to a laboratory to examine and measure them in detail. It is important to know what variations can be expected in different geographic areas in terms of the range of crystal shapes and sizes. A cryosystem has been developed [4] to preserve snow crystals collected in the field so that they can be imaged using low-temperature scanning electron microscopy (SEM). This technique uses liquid nitrogen as a coolant and special precooled dewars to store and transport the snow crystal samples, which are virtually undisturbed, to the SEM laboratory in Beltsville, MD. The goal of this study is to determine, through a combination of field work and modeling, how the shape of snow crystals affects the response of microwave radiation emanating from below and within the snowpack. Ultimately, this information should be useful in producing more reliable snow cover and snow depth algorithms.

II. EXPERIMENT SETUP

Snow crystal samples have been collected and examined from snowpacks on the North Slope of Alaska, in the Rocky Mountains of Colorado and Wyoming, in the Cascade Range in Washington, in the Appalachian Mountains of West Virginia, and in north-central Wisconsin. Each of these areas represents a different physiographic and subclimatic region, having different snow conditions.

The crystals were collected from the walls of snow pits. A specially fabricated snow sample holder was covered with a thin layer of methyl cellulose solution (Tissue Tek) and placed near the snow pit wall. Snow crystal samples from a selected layer of the snowpack were gently dislodged from the pit wall and collected on the surface of the sample holder. Each of the collected crystals fit into one of several standard shapes. Fig. 1 shows two examples of SEM images of differently shaped snow crystals collected *in situ*. After obtaining a visible accumulation of snow crystals, the holder was plunged into a styrofoam reservoir containing liquid nitrogen (LN₂) at -196°C and transferred to a square profile, brass tube for low temperature storage during shipping. Once filled with sample holders, the brass tubes are placed in dry shipping dewars at liquid nitrogen temperatures and shipped to Beltsville for analysis. The Alaskan samples were in transit to Beltsville, for seven days, but the dewars maintained a temperature of -196°C , and the samples generally appeared to be undisturbed upon observation (for more information on this technique, see [5]).

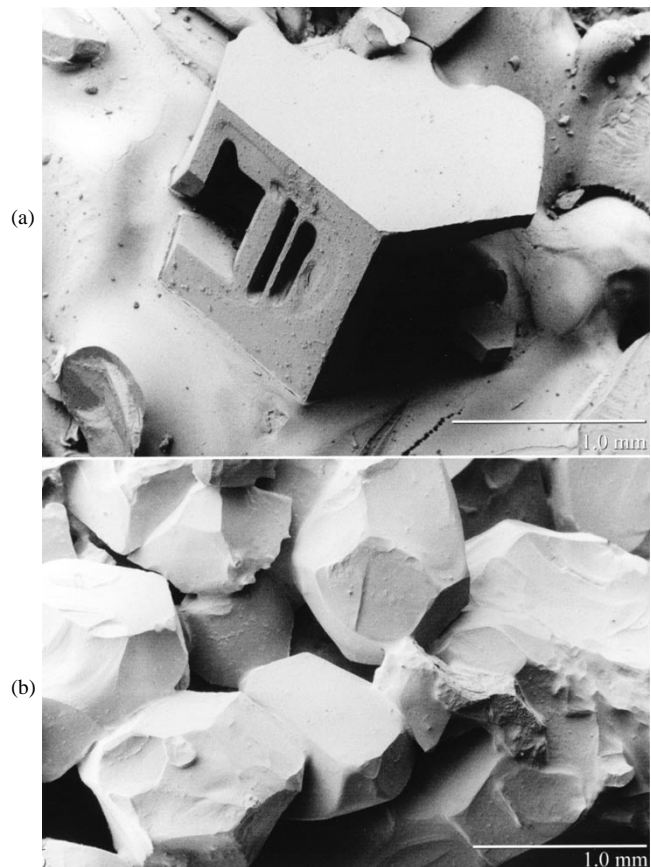


Fig. 1. (a) Scanning electron microscope image of an angular depth hoar crystal. (b) Scanning electron microscope image of snow grains.

III. MODELING

In terms of modeling snow crystals, although it may be that spheroids are adequate substitutes for actual snow and ice particles in radiative transfer calculations, it is not known with a high degree of certainty whether differently shaped crystals of a given size range will affect how microwave radiation is scattered. To address this concern, a discrete dipole model [6] is used to approximate the scattering of idealized snow crystals having various shapes. The shapes can be cubic, cylindrical, etc., or clusters of two or more crystals, and they are modeled as an array of point dipoles. The electromagnetic scattering problem for the arrays is then solved, essentially, exactly using a Fortran program called DDSCAT [6].

DDSCAT is very versatile and can be used to approximate the scattering from snow crystals or even interstellar dust. The version of the program used here uses the discrete dipole approximation formulas [7]. The code incorporates fast Fourier transform methods [8].

For this DDSCAT program, the wavelength selected was 8100 microns (0.81 cm), corresponding to 37 GHz. Studies have shown [3] that, for snowpacks less than a meter in depth, more information about the SWE can be derived when using a frequency of about 35 GHz than when using higher or lower frequencies. A refractive index of 1.78 is used for the real part of the refractive index of ice, and 0.0024 is used for the imaginary part (the refractive index is the square root of the dielectric constant). Particles were modeled having an effective radius (radius of a sphere of equivalent volume) of 0.1, 0.3, 0.5, 0.7, and 0.9 mm. The shapes modeled included spheroids, ellipsoids, cylinders, cubes, tetrahedrons (four-sided pyramid), and hexahedrons. There are three different target

TABLE I
EXTINCTION EFFICIENCY FOR DIFFERENT CRYSTAL SHAPES AND SIZES

	0.1 mm	0.3 mm	0.5 mm	0.7 mm	0.9 mm
sphere	3.273×10^{-4}	2.398×10^{-3}	1.307×10^{-2}	4.772×10^{-2}	1.307×10^{-1}
ellipsoid	2.937×10^{-4}	2.134×10^{-3}	1.137×10^{-2}	4.023×10^{-2}	1.064×10^{-1}
cylindrical	3.066×10^{-4}	2.218×10^{-3}	1.176×10^{-2}	4.139×10^{-2}	1.086×10^{-1}
hexahedron	3.351×10^{-4}	2.248×10^{-3}	1.310×10^{-2}	4.734×10^{-2}	1.282×10^{-1}
tetrahedron	3.981×10^{-4}	2.910×10^{-3}	1.601×10^{-2}	5.940×10^{-2}	1.658×10^{-1}
cube	3.483×10^{-4}	2.518×10^{-3}	1.361×10^{-2}	4.927×10^{-2}	1.336×10^{-1}

size is the radius of the particle in mm
wavelength is equal to 8100 microns or 0.81 cm
refractive index is $1.78 + 0.0024i$

orientations with calculations for two incident polarization states. In this study, randomly oriented dipoles are specified. Scattered intensities are computed for two scattering planes at intervals of 30° in the scattering angle theta: $\phi = 0$ for the $x-y$ plane, and $\phi = 90$ for the $x-z$ plane.

Using the discrete dipole model for spheroid crystals with an effective radius of 0.3 mm, for example, and with the above inputs, the average scattering is equal to 1.431×10^{-2} , the average absorption is equal to 9.665×10^{-4} , and the extinction efficiency is equal to 2.398×10^{-3} ($Q_{\text{extinction}} = Q_{\text{scattering}} + Q_{\text{absorption}}$). This compares favorably to Mie calculations (also with a radius of 0.3 mm), which give a value for extinction efficiency of 1.40×10^{-3} . Table I provides extinction efficiency values for the six different shapes and five different particle sizes. It can be seen that there are only very small differences between results for spherical crystals and crystals having other shapes. In general, the hexahedron is closest to the spheroid in terms of extinction efficiency and the ellipsoid and tetrahedron are furthest. The size of the crystal has little consequence on how different shapes scatter microwave energy.

IV. DISCUSSION

Finding a representative grain size, shape, and density to relate to microwave extinction properties is crucial to improving remote sensing and model performance. It has been shown ([9] among others) that the equivalent sphere seems to be best chosen as the shape with the same surface-to-volume ratio as real snow grains, which are nonspherical scatterers. Recently published research [9]–[11] has demonstrated the role of grain size and effective or equivalent grain size in scattering passive microwave energy. In most cases, this work has considered only spheroid or ellipsoid shapes. Are these rounded snow grains appropriate to use as the average crystal shape when modeling microwave scattering and absorption?

The microwave radiation emitted by a snowpack is dependent on the physical temperature, crystal characteristics, and density of the snow. A basic relationship between these snow properties and the emitted radiation can be derived by using the radiative transfer approach. The lack of precise information about snow crystal size and shape is compensated for by using an average size of 0.3 mm (radius), a density of 300 kg m^{-3} , an assumed spherical shape for the snow crystals, and the assumption that the crystals scatter radiation

incoherently and independently of the path length between scattering centers. These quantities are then used in radiative transfer equations to solve the energy transfer through the snowpack. If the crystals differ significantly from the averages and assumptions, poor SWE values will result.

The effects of shape on extinction efficiency can be used as a measure of the effectiveness of different shaped scatterers. It was shown [12] that the extinction response for a cylinder was somewhat higher, though not significantly different from that of a sphere. Modeling of other shapes give more credence to this observation.

When examining snow crystals in the field with a magnifying lens, it is apparent that they consist of a myriad of shapes and sizes. Because the edges or branches are quickly worn off, the shapes become more and more rounded as the snow season progresses. The process of freezing and thawing (metamorphism) further rounds the crystals. Thus, the spherical shape used in the radiative transfer approximations is not unrepresentative of what is observed in the field. Of course, when viewed with an electron microscope, the detail is so great that individual crystals can be assigned a specific shape, but the variation between even adjacent crystals can be substantial. Regardless, though, the size of the crystal and the effective particle size [9] are so dominant in scattering that the cumulative contribution of other structural features, such as shape, is overwhelmed.

V. CONCLUSIONS AND FUTURE PLANS

While crystal size and effective crystal size are strongly related to microwave brightness temperature, it appears from the modeling results of this study that the shape of the snow crystal is of little consequence in accounting for the transfer of microwave radiation (at 0.81 cm) from the ground through the snowpack. In addition to crystal shape, variations in the positioning [13] and orientation of crystals in a snowpack will be modeled to assess what effect these properties have on volume scattering. Also, the DDSCAT model will be run for a range of incident angles to examine what effect, if any, is evident in the scattering cross section and the extinction efficiency.

ACKNOWLEDGMENT

The authors would like to thank Dr. C. Benson, Dr. R. Armstrong, Dr. G. Liston, Dr. M. Sturm, Dr. A. Klein, Dr. E. Josberger, and T. Cruickshank for their help in collecting and analyzing snow crystals. Also, J. Chien and J. Barton need to be recognized for assistance in running the DDSCAT model.

REFERENCES

- [1] J. Hallett, "Freeze frame," *Sciences*, pp. 22–26, Nov./Dec. 1996.
- [2] T. Schmugge, "Techniques and applications of microwave radiometry," in *Remote Sensing of Geology*, B. Siegal and A. Gillespie, Eds. New York: Wiley, 1980, pp. 337–352.
- [3] A. T. C. Chang, J. L. Foster, and D. K. Hall, "Nimbus-7 SMMR derived global snow cover parameters," *Ann. Glaciol.*, vol. 9, pp. 39–44, 1987.
- [4] W. P. Wergin, A. Rango, and E. F. Erbe, "Observations of snow crystals using low-temperature scanning electron microscopy," *Scanning*, vol. 17, pp. 41–49, 1995.
- [5] A. Rango, W. P. Wergin, and E. F. Erbe, "Snow crystal imaging using scanning electron microscopy, Part II—Metamorphosed snow," *Hydrol. Sci. J.*, vol. 41, pp. 231–250, 1996.
- [6] B. Draine and P. Flatau, "Discrete dipole approximation for scattering calculations," *J. Amer. Opt. Soc.*, vol. 11, pp. 1491–1499, 1994.
- [7] B. Draine, "The discrete dipole approximation and its application to interstellar graphite grains," *J. Astrophys.*, vol. 33, pp. 848–872, 1988.
- [8] J. Goodman, B. Draine, and P. Flatau, "Applications of FFT techniques to the discrete dipole approximation," *Opt. Lett.*, vol. 16, pp. 1198–1200, 1991.
- [9] C. Matzler, "Autocorrelation functions of granular media with arrangement of spheres, spherical shells or ellipsoids," *J. Appl. Phys.*, vol. 3, pp. 1509–1517, 1997.

- [10] J. Shi, R. Davis, and J. Dozier, "Stereological determination of dry snow parameters for discrete-scatterer microwave modeling," *Ann. Glaciol.*, vol. 17, pp. 295–299, 1993.
- [11] L. Tsang, K. Ding, and S. Shih, "Monte Carlo simulations of scattering of electromagnetic waves from dense distributions of nonspherical particles," in *Proc. IGARSS*, Singapore, 1997, pp. 919–921.
- [12] J. Foster, D. Hall, A. Chang, A. Rango, W. Wergin, and E. Erbe, "Observations of snow crystal shape in cold snowpacks using scanning electron microscopy," in *Proc. IGARSS*, Lincoln, NE, 1996, vol. 4, pp. 2011–2013.
- [13] P. R. Siqueira, K. Sarabandi, and F. T. Ulaby, "Numerical simulation of scatterer positions in a very dense medium with an application to the two-dimensional Born approximation," *Radio Sci.*, vol. 30, no. 5, pp. 1325–1338, 1995.

Smoothing Effect of Wavelet-Based Speckle Filtering: The Haar Basis Case

Seisuke Fukuda and Haruto Hirose

Abstract—The smoothing effect of the wavelet-based speckle filtering that we proposed is investigated. The filtering reduces the amplitude of wavelet coefficients, and a theoretical investigation with the Haar basis derives a functional relation between the ENL and two parameters: the wavelet level and the degree of the amplitude reduction.

Index Terms—Speckle reduction, speckle wavelet, synthetic aperture radar (SAR).

I. INTRODUCTION

Synthetic aperture radar (SAR) images are inherently accompanied with speckle as a result of coherent illumination. In general, speckle in SAR images is regarded as undesirable noise since its existence damages radiometric resolution and makes scene analysis difficult. The origin of speckle and its statistics have been extensively investigated for the last several decades. Speckle is generated by interaction of reflected waves from various independent scatterers within a resolution cell [3]. When the number of scatterers is large, speckle is fully developed, and the scattered field amplitude obeys a Rayleigh distribution, so that the intensity obeys an exponential distribution. In the case of high-resolution data, including only a small number of scatterers in a cell, however, the field amplitude distribution has non-Rayleigh characteristics [4].

Speckle reduction is of great concern in SAR remote sensing. The first step of speckle reduction is multilook processing, which is based on the incoherent summation of independent frames of the same scene. Multilook processing smooths speckle at the cost of spatial resolution. Numerous postmultilook adaptive filters to reduce speckle have been proposed in the past; the Lee filter [5], the Kuan filter [6], the Frost filter [7], the sigma filter [8], the Gamma-Gamma MAP filter [9], and so on. The ultimate goal, though difficult to reach,

of these adaptive filters is that speckle is smoothed, while textural information and structural features, such as edges are preserved.

Wavelet technique has been variously applied to image processing since the multiresolution analysis theory was developed in the second half of the 1980's [12], [13]. In the field of remote sensing, wavelet-based multiresolution analysis is also a promising method [14]. As a wavelet denoising method, wavelet shrinkage [15], often referred to as hard/soft thresholding, is well known; wavelet shrinkage is based on a policy of thresholding wavelet coefficients toward zero in each wavelet domain. We have proposed an alternative approach that "reduces" or "compresses" the amplitude of wavelet coefficients, and we have successfully applied it to SAR images [1], [2].

The smoothing effect of our wavelet-based speckle filtering depends on the wavelet subspaces level (i.e., the number of transformation) and the degree of the amplitude reduction of wavelet coefficients [1], [2]. These parameters have to be set according to user's desirable smoothing effect. In this paper, following a brief review of the method, a quantitative consideration of its smoothing effect, where the Haar basis is used, is given. The consideration facilitates the settlement of parameters. Furthermore, we refer to the case in which a SAR image is logarithmically transformed before the wavelet-based filtering. This scheme is known as homomorphic processing [16], taking account of the multiplicative property of speckle.

II. WAVELET-BASED SPECKLE FILTERING: A REVIEW

A. Multiresolution Analysis

Before reviewing the wavelet-based speckle filtering that we have proposed, we survey Mallat's multiresolution analysis theory [12], [13] in this subsection.

The multiresolution analysis was originally developed as a tool for systematical construction of an orthonormal wavelet ψ . A multiresolution analysis is defined by a scaling function ϕ and a sequence of closed subspaces $\{V_j | j \in Z\}$, which approximate the space $L^2(R)$ of R -periodic square-integrable functions, with the following properties:

- 1) $V_j \subset V_{j+1}$ ($j \in Z$);
- 2) $\bigcup_{j \in Z} V_j$ is dense in $L^2(R)$;
- 3) $\bigcap_{j \in Z} V_j = \{0\}$;
- 4) $f(x) \in V_j \Leftrightarrow f(2^{-j}x) \in V_0$;
- 5) the collection $\{\phi(x-k) | k \in Z\}$ is an orthonormal basis of V_0 ; an orthonormal basis has the norm normalized to one.

From 4) and 5), it follows that the family obtained by dilations and translations of ϕ

$$\phi_{j,k} = 2^{j/2} \phi(2^j x - k), \quad (j, k \in Z) \quad (1)$$

is an orthonormal basis of V_j . Since $\phi \in V_0 \subset V_1$ [by 1) and 5)], we have the "two-scale relation" of the scaling function ϕ

$$\phi(x) = \sum_{k \in Z} p_k \phi(2x - k) \quad (2)$$

where $\{p_k \in l^2\}$ is called the "two-scale sequence," which relates $\phi(x)$ with the functions $\phi(2x - k)$. Now, let us consider the orthocomplement W_j of V_j in V_{j+1} (i.e., $V_j \perp W_j$, $V_j \oplus W_j = V_{j+1}$). If we define $\psi(x)$, similarly to (1) and (2), as

$$\psi(x) = \sum_{k \in Z} q_k \phi(2x - k) \quad (3)$$

Manuscript received October 6, 1997; revised June 23, 1998.

The authors are with the Institute of Space and Astronautical Science, Sagami-hara, Kanagawa, 229-8510 Japan (e-mail: fukuda@atom.eng.isas.ac.jp).

Publisher Item Identifier S 0196-2892(99)01182-1.